ZnCdO: Status after 20 years of research

Jesus Zúñiga-Pérez

ZnCdO: status after 20 years of research

Jesús Zúñiga-Pérez

CRHEA-CNRS, Rue Bernard Grégory, 06560 Valbonne, France

jzp@crhea.cnrs.fr

Abstract:

With the increasing attention devoted to ZnO in the late nineties, the discovery of ZnCdO as a means of reducing its bandgap towards visible wavelengths promised it a bright future in optoelectronics, which should run in parallel to its possible applications as a transparent conducting oxide. This review will cover the developments achieved so far in the growth of ZnCdO, in the understanding of its structural properties, paying special attention to the *competition* between wurtzite and rocksalt phases, as well as in the analysis of its optical and electronic properties. Finally, some of the devices demonstrated with ZnCdO will be reviewed together with the difficulties they have encountered.

Introduction

As of today, the success of GaN-based optoelectronic devices relies on the combination of GaN and InGaN in quantum heterostructures, which have enabled the fabrication of commercially available light-emitting diodes and laser diodes. Indeed, InGaN allows tuning the bandgap of GaN far into the visible and even into the infrared, and has enabled the development of quantum wells displaying internal quantum efficiencies larger than 90%.[1]

In the late 90's, ZnO was "rediscovered once again"[2] and was introduced as an interesting alternative to GaN, given the numerous structural, optical and electronic properties shared by the two materials. In this context, ZnCdO appeared as the optimum candidate to play the role of InGaN, given that the introduction of Cd into the wurtzite ZnO lattice was shown to reduce the bandgap from the UV down into the visible.[3] Besides, it was soon found that ZnMgO and ZnCdO alloys grown along the polar *c*-direction could be lattice matched, as in both systems the *a* lattice parameter increases with increasing Mg (or Cd) concentration.[3] This generated an enormous optimism and offered new opportunities to the ZnMgO/ZnCdO system in terms of bandgap engineering with negligible, eventually null, strain accumulation. This situation contrasted with that found in the AlGaN/InGaN system. However, contrary to the III-nitrides system in which all binary compounds crystallize in the hexagonal wurtzite structure, the extreme binary compounds MgO and CdO display a cubic thermodynamically stable phase, rocksalt, that is different from the wurtzite one of ZnO. Indeed, it was rapidly understood that this could impose some limitations in terms of Cd (and Mg) solubility as well as in terms of crystalline quality,[3] aspects that will be specifically reviewed in the following pages.

In parallel to the development of ZnCdO as "active" material in optoelectronic devices, and in most cases independently of, this compound has been investigated as a "passive" transparent conducting oxide (TCO). The first report on ZnCdO studied as a TCO dates back to 1996,[4] i.e. 2 years before it was introduced to the optoelectronic community.[5] As such, it has been considered as a possible alternative to ITO, similarly to highly-doped ZnO, CdO or SnO_2,[6,7,8] though with much less success than some of its competitors. As for the optoelectronic field, the first report of 1996 already identified the structural incompatibility between wurtzite ZnO and rocksalt CdO.[4] However, the

requirements in terms of crystalline quality for TCO applications being less stringent than for optoelectronic devices, the groups working in this topic have contributed decisively to achieve single-phase ZnCdO across the full composition range, as will be discussed hereafter.

In this context, a full range of growth techniques has been used to grow ZnCdO with controlled structural, optical and electronic properties, going from more sophisticated ones, such as molecular beam epitaxy (MBE) or metalorganic vapour phase epitaxy (MOVPE), to more simple and cheaper ones, such as solid state sintering or magnetron sputtering. In the following we will review, briefly, their accomplishments as well as the encountered difficulties, especially when characterizing different phases or when studying composition homogeneity. The review is organized as follows: first we will address the phase separation issue and the alloy composition homogeneity, two aspects often related to each other. This will allow us to introduce the employed growth techniques and discuss how it has been possible to achieve any desired alloy composition. In the second part we will introduce the optical and electronic properties of ZnCdO, both in the wurtzite and in the rocksalt phase. Finally, we will introduce some of the applications that were envisaged for ZnCdO, and in some cases partially achieved, and will end with an outlook on what might wait in the near future.

Growth of ZnCdO: Wurtzite Vs Rocksalt.

It was known in the late nineties that the thermodynamically-stable crystalline phases of ZnO (wurtzite) and of CdO (rocksalt) were different.[9] Thus, a phase transition from hexagonal to cubic material could be expected in ZnCdO when going from pure ZnO to pure CdO, and might result eventually in phase separation within the films. This is probably one of the reasons why in many of the first reports the Cd concentrations in the ZnCdO films were relatively low (see Table 1), typically below 10% or less.[3,51011,12,13,14,15,16,17] When increasing the Cd concentrations by a few percents, noticeable effects were observed in the structural and/or optical properties. These included the strong increase in the full width at half maximum of the symmetric rocking curve[3] or the appearance of additional peaks in diffraction patterns[16] obtained in transmission electron microscopy. In some cases the appearance of secondary phases, i.e. rocksalt inclusions in a wurtzite matrix, was preceded by composition fluctuations. The fluctuations could be large enough to give rise to resolved contributions of ZnCdO alloys with different Cd contributions both in structural (e.g. in $2\theta/\omega$ scans)[15] and optical measurements (e.g. in photoluminescence or cathodoluminescence measurements),[13,14] as shown in Figure 1.

It soon became clear that for each combination of growth technique/orientation (compare references 13, 14, and 15), or growth technique/substrate-growth conditions (compare references 3 and 18), the Cd concentrations for which strong composition fluctuations appeared were different, pointing towards a strong sensitivity of Cd incorporation to the growth environment. It should be noted that, hopefully enough, most reports on ZnCdO films employed the same characterization techniques to determine the Cd concentration on the alloy, the most common ones being Rutherford backscattering (RBS), secondary ion mass spectrometry (SIMS) and energy-dispersive x-ray spectroscopy (EDX), enabling fair comparison between different articles (see Table 1). Unfortunately, the equivalence between the Cd concentrations determined by several techniques has been rarely reported, as done in reference 19 for RBS and SIMS.

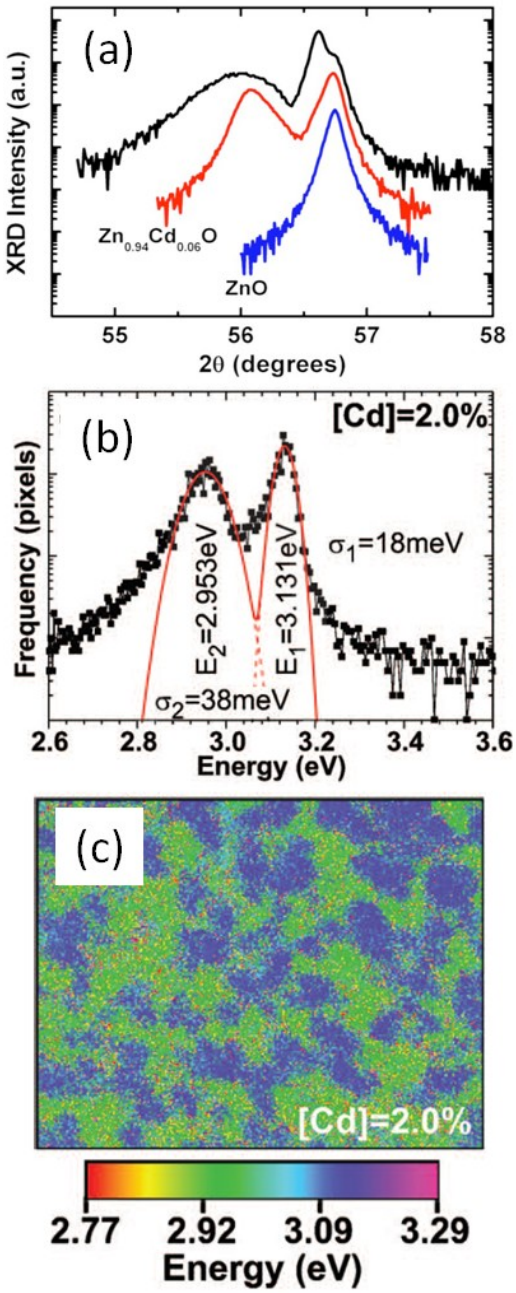

Figure 1: Examples of Cd concentration fluctuations below the critical Cd concentration for the wurtzite to rocksalt phase transition. (a) $2\theta/\omega$ scans of MOVPE-grown ZnO and ZnCdO thin films, exhibiting distinctive Cd composition fluctuations for Cd concentrations above about 8%. From reference 15, with the permission of AIP Publishing. (b) and (c) CL wavelength image and matching histogram for an MOVPE-grown ZnCdO film with a Cd concentration of about 2%. From reference 14, with the permission of AIP Publishing.

As pointed out as early as 1998,[5] the fact that for a given temperature the vapor pressure of CdO is significantly larger than that of ZnO might lead to a reduction of the Cd concentration in the alloy with respect to the nominal Zn/Cd ratio in the gas-phase or in the plasma. This suggests that a way to increase Cd composition can be the reduction of the growth temperature, which was tested with success in 2006 by MBE:[20] single-phase (wurtzite) ZnCdO alloys with up to 32% Cd could be grown at temperatures as low as 150°C. Interestingly, the buffer layer employed was ZnMgO with a Mg content of 10% that contributed to reducing the lattice mismatch[3] and provided a high-quality wurtzite template to deposit the ZnCdO on, both in terms of surface roughness and structural

quality. Sadofev *et al*.[20] were extremely careful in determining the phase purity (i.e. pure wurtzite) of their films, which they assured by performing pole figures measurements on asymmetric rocksalt reflexes whose symmetry is easy to differentiate from that of hexagonal ones.[21,22] Indeed, measuring just symmetric $2\theta/\omega$ scans might be misleading, as the rocksalt and wurtzite diffractions peaks might overlie and, thus, the signal from a preponderant phase might mask the existence of other phases.

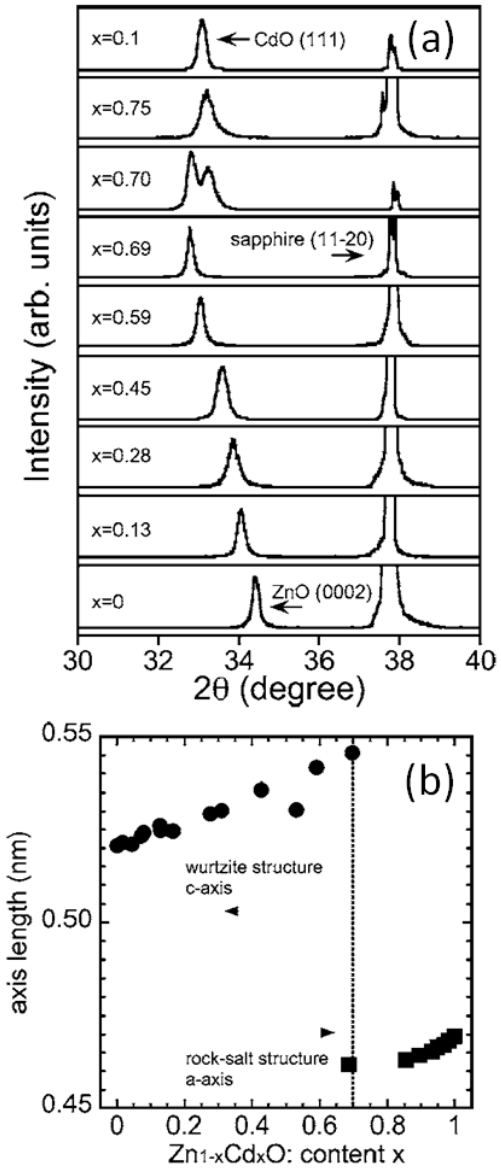

Figure 2: (a) $2\theta/\omega$ scans of RPE-MOVPE-grown ZnCdO thin films on a-sapphire spanning the whole composition range, from pure ZnO to pure CdO. (b) Lattice parameter parallel to the growth direction as a function of Cd composition (c-lattice paramtere for wurtzite ZnCdO and a lattice parameter for rocksalt ZnCdO). From reference 23, with the permission of AIP Publishing.

The same year, in 2006, a major breakthrough was achieved by the group of J. Temmyo at Shizuoka University: they reported the continuous tuning of the Cd composition across the entire composition range, enabling them to determine the critical Cd concentration for the wurtzite-to-rocksalt phase transition at about 70%.[23,24] Two aspects were necessary for them to succeed: first, they employed growth temperatures in the range 250°C-450°C, slightly higher than those of Sadofev

et al.;[20] second and most important, they employed a remote plasma-enhanced MOVPE (RPE-MOVPE) system that they had introduced three years before for the growth of pure ZnO[25] and successfully applied to wurtzite ZnCdO in 2004.[26] Indeed, credit should be given to this last work on wurtzite ZnCdO and the associated optical and structural characterizations,[27] whose importance was rapidly overshadowed by their own work compiling the growth and properties of ZnCdO across the full composition range.[23] As shown in Figure 2(a), a single peak associated with the wurtite ZnCdO phase was observed for concentrations smaller than 70%, shifting continuously towards smaller 2θ angles with increasing Cd content. At a concentration of about 70% two peaks are clearly distinguished, corresponding to wurtzite and rocksalt ZnCdO phases coexisting within the films. For larger Cd concentrations, only one peak displaying again a continuous shift with varying Cd concentration is detected, but this time associated to rocksalt ZnCdO. The continuous evolution of the *c* and *a* lattice parameters as a function of Cd concentration, for the wurtzite and rocksalt phases respectively, is displayed in Figure 2(b). In the following years, the critical Cd concentration for the wurtzite-to-rocksalt phase transition was confirmed to be in the range 67%-70% by other growth techniques.[28,29,30]

At the same period of time, new calculation schemes were introduced to analyze the stability of isovalent but heterostructural alloys such as MgO-ZnO.[31] These theoretical approaches were subsequently applied to the CdO-ZnO system[32,33] and further extended by taking into account all possible clusters configurations,[34] which should enable to emulate different growth conditions and, thus, establish conclusions on phase stability as a function of growth conditions. Overall, theoretical calculations confirm that the local bonding configuration (four-fold or six-fold coordination) depends more on the actual growth conditions for ZnCdO than for ZnMgO,[34] which might explain why in Table I there is such a big dispersion in terms of composition fluctuations/phase stability/pure crystalline phases.

Growth technique	Substrate	Composition $Zn_{1-x}Cd_xO$ ($0\leq x\leq 1$)	Composition measurement technique	Phases	Comment	Reference	Related Publications
MBE	a-sapphire	<0.05	Auger	-	Composition fluctuations	11	1
MBE	a-sapphire	0.07<x<0.18	Micro-EDX	-	Composition fluctuations	12	1
MBE	ZnO on GaN on sapphire	x~0.02 x~0.09 x~0.16	RBS	Wurtzite		16	2
MBE	ZnO on GaN-on-sapphire	x~0.09 x~0.16	RBS	wurtzite	Composition/phase fluctuations	17	2
MBE	ZnMgO on sapphire	≤0.32	EDX	wurtzite		20	3
MBE	O-polar ZnO and a-sapphire	≤0.17	EDX	wurtzite		35	3
MBE	O-polar ZnO and a-sapphire	≤0.19	EDX	wurtzite	Thermal stability	36	3
MBE	ZnO on c-sapphire	≤0.13	EDX	Wurtzite and rocksalt	Thermal stability and phase transition (x~0.08)	37	
MBE	ZnO on c-sapphire	x~0.02				38	4
MBE	ZnO on c-sapphire	0.1≤x≤0.20	EDX			39	4
MOVPE	ZnO on GaN-on-sapphire	<0.05	XRD	wurtzite	Composition fluctuations	13	5
MOVPE	ZnO on GaN-on-	<0.02	XRD	wurtzite	Composition	14	5

	sapphire				fluctuations		
MOVPE	ZnO on c-sapphire	x~0.07	RBS and SIMS	wurtzite	Thermal stability	19	6
MOVPE	r-sapphire	≤0.06	SIMS			40	
MOVPE	r-sapphire	≤0.09	RBS	Wurtzite	Composition fluctuations	15	
MOVPE	c-sapphire	0≤x≤0.60	RBS	Wurtzite, zincblende, and rocksalt	Phase separation	41	6
MOVPE	Zn- and O-polar ZnO	x≤0.03	Comparison with literature (PL)	Wurtzite	Growth on opposite polarities	42	
RPE-MOVPE	a-sapphire	0≤x≤0.70	EPM	Wurtzite		26	7
RPE-MOVPE	a-sapphire	0≤x≤0.70	EPM	Wurtzite		27	7
RPE-MOVPE	a-sapphire	x~0.04 x~0.08	EPM	Wurtzite		43	7
RPE-MOVPE	a-sapphire	0≤x≤1	EPM and AAS	Wurtzite and rocksalt	Phase transition (x~0.7)	23	7
RPE-MOVPE	a-sapphire	0≤x≤1	AAS	Wurtzite and rocksalt	Phase transition (x~0.7)	24	7
RPE-MOVPE	ZnO on a-sapphire	x~0.15		Wurtzite	MQWs	44	7
RPE-MOVPE	ZnO on a-sapphire	x≤0.60	ASS	Wurtzite	Alloy broadening	45	7
PLD	c-sapphire and (0001) SCAM	x≤0.07	EPM and ICP-OES	Wurtzite	Composition fluctuations	3	8
PLD	(0001) SCAM	x~0.04		Wurtzite	MQWs	10	8
PLD	ZnO on a-sapphire	x≤0.04	Comparison with literature (PL)	Wurtzite	Thermal stability	46	
PLD	a-sapphire	x≤0.25	EDX	Wurtzite		18	
PLD	c-sapphire	x≤0.09	EDX	Wurtzite		47	
PLD	quartz	-	-	Wurtzite	Band offsets	48	
PLD	ZnO on c-sapphire	x~0.08	EDX	Wurtzite	MQWs	49	
PFCAD	Glass	0≤x≤1	RBS	Wurtzite and rocksalt	Phase transition (x~0.69)	28	9
PFCAD	Glass	0≤x≤1	RBS	Wurtzite and rocksalt	Phase transition (x~0.69)	29	9
DSRFMS	Glass	0.21≤x≤0.68	RBS	Wurtzite and rocksalt	Phase transition (x~0.67)	30	
RF magnetron sputtering	quartz	x~0.6	EDX	Rocksalt, zincblende and wurtzite	Thermal stability	50	
DC magnetron sputtering	Si	x~0.1 x~0.52	ICP-AES	Wurtzite and rocksalt	Thermal stability	51	10
DC magnetron sputtering	Si and quartz	x≤0.78	ICP-AES	Wurtzite and rocksalt	Composition fluctuations and phase transition (x~0.78)	52	10
Spray pyrolysis	Glass	-	-	Wurtzite and rocksalt	Phase transition	53	
SRR	-	x≤0.14	-	Wurtzite and rocksalt	*Electronic structure*	54	

Table 1*: ZnCdO thin films growth approaches found in the literature, with the studied Cd concentrations, experimental techniques to determine the Cd concentration as well as the crystalline phases detected (if analyzed). The last column indicates articles devoted to the same or very similar samples by the same research groups.*

Before addressing the optical and electronic properties of ZnCdO it is worth noting that compared to ZnO,[55,56,57] the number of reports on the growth and characterization of ZnCdO nanowires (or nanorods) is much smaller, as compiled in Table 2.

Growth technique	Substrate	Catalyst	Composition $Zn_{1-x}Cd_xO$ ($0 \le x \le 1$)	Composition measurement technique	Phases	Size	Reference	Related publications
Thermal evaporation		-	x≤0.02	EDX	Wurtzite	diameter~20 nm	58	
VPE	Si(100)	Au	x≤0.17	EDX	Wurtzite	diameter~150nm	59	1
VPE	Si(100)	Au	x≤0.17	EDX	Wurtzite	diameter~150nm	60	1
VPE	Si(100)	Au	x~0.17 x~0.07	EDX and XPS	Wurtzite	diameter~150nm	61	1
PLD	ZnO microwires grown by VPE	-	x~0.24	EDX	Wurtzite	500nm≤diameter≤50μm	62	
CVD	GaN on sapphire	-		EDX	Wurtzite	200nm≤diameter≤400nm	63	
RPE-MOCVD	a-sapphire	-	x≤0.45	Micro-EDX	Wurtzite	100nm≤diameter≤200nm	64	2
RPE-MOCVD	a-sapphire	-	x~0.54 0.06≤x≤0.14 0.20≤x≤0.27	Micro-EDX	Wurtzite	diameter~70 nm	65	2
VPE	-	-	x≤0.08	Micro-EDX and XPS	Wurtzite	diameter~20 nm	66	
ECD	F-doped SnO2 on glass and GaN on sapphire	-	x≤0.44	EDX	Wurtzite and rocksalt (phase separation)	diameter~100 nm	67	

Optical properties of ZnCdO.

The optical properties of ZnCdO alloys have been studied by a number of techniques, including photoluminescence, absorption, transmission, cathodoluminescence and ellipsometry. As illustrated in Figure 3, absorption measurements across the full composition range as well as photoluminescence of wurtzite ZnCdO show clearly the narrowing of the bandgap with increasing Cd content.

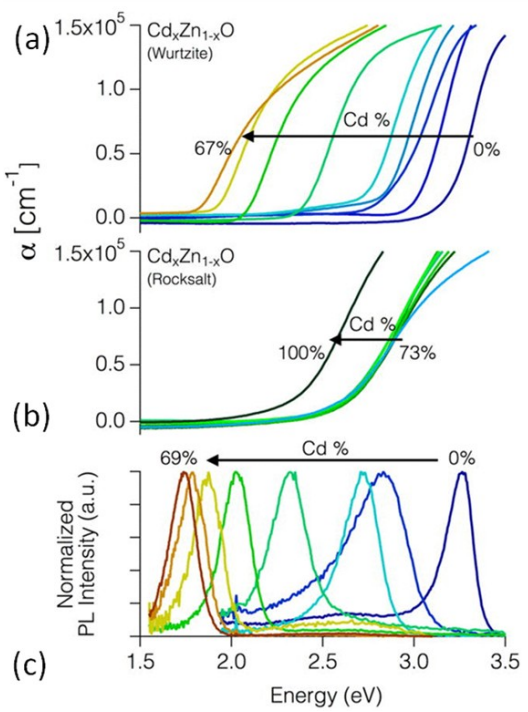

Figure 3: Optical absorption coefficients as a function of photon energy of (a) wurzite ZnCdO, and (b) rocksalt ZnCdO, along with (c) photoluminescence spectra of wurtzite ZnCdO thin films measured at room-temperature. From reference 28, with the permission of AIP Publishing.

As for many semiconductor alloys,[68] the intrinsic bandgap of wurtzite ZnCdO ($Zn_{1-x}Cd_xO$) displays a nonlinear quadratic dependence on Cd concentration that can be described by a bowing parameter *b*:

It should be noted that in the previous equation the intrinsic bandgaps of the two extreme binaries that appear correspond to those of their wurtzite phases. This implies that we can in principle determine the bandgap of CdO in its wurtzite form, which was calculated in the early 2000s to be in the order of 1.5eV.[69] One should be careful when applying/comparing this equation to the experimental data in the literature, given that often excitonic contributions to the band edge have been neglected,[3,43] leading to an underestimation of the ZnO bandgap, and given that in general bandgap renormalization and carrier-filling effects (i.e. Moss-Burstein effect) do not have been taken into account. As shown first for CdO,[70] these two last effects need to be considered if reliable bandgap values are to be determined, especially for large Cd content ZnCdO alloys. This is clearly shown in Figure 4 (a), where the dependence of photoluminescence emission, absorption edge (as extracted from α^2 Vs energy fittings, where α is the absorption coefficient) and intrinsic bandgap (i.e. removing renormalization and Moss-Burstein contributions) are plotted as a function of Cd concentration. As already stated, the difference between absorption edge and intrinsic bandgap becomes non-negligible for Cd contents above 40%. From these data the authors extracted a bowing parameter of 0.94 eV,[28] very similar to a previous value of 0.95eV determined with samples in the low-Cd content range (up to 16% of Cd).[16] These bowing parameters seem to be more accurate than larger values determined either with few experimental points (5.93 eV),[3] or with fits giving values for the wurtzite CdO bandgap as large as 2.7eV.[52]

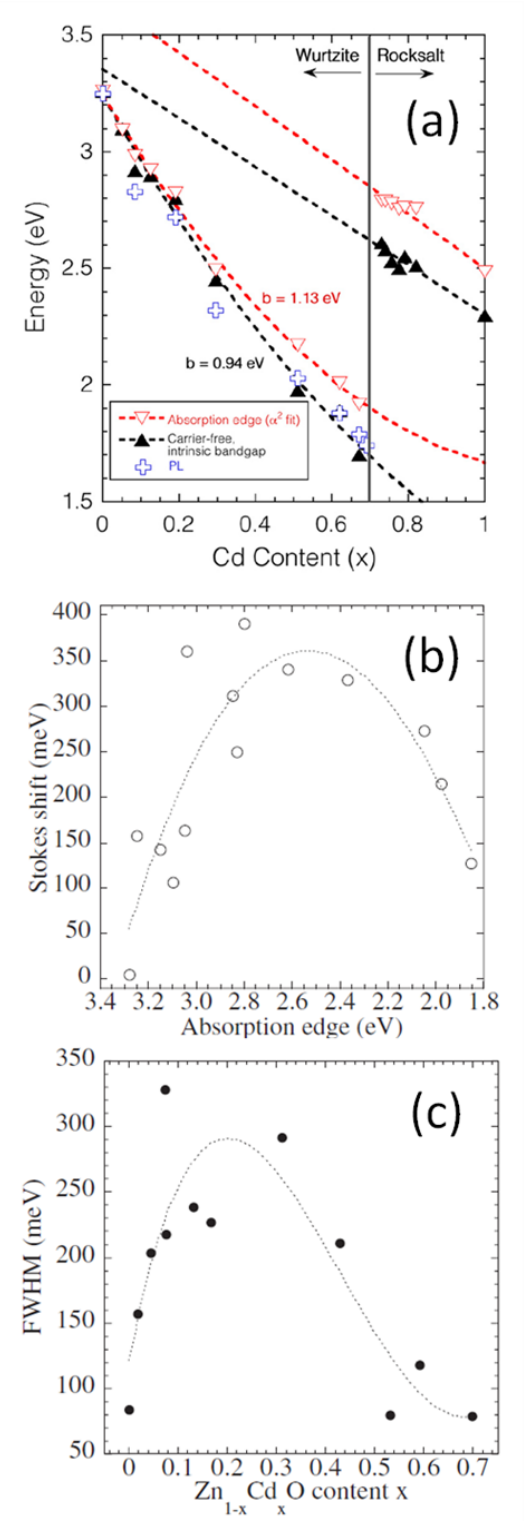

Figure 4: (a) Near-band edge photoluminescence, direct-gap absorption edge extrapolated from linear α^2 Vs energy plots, and intrinsic bandgap (i.e. removing carrier-filling and carrier-induced renormalization) as a function of Cd content across the full composition range measured on thin films deposited by cathodic arc deposition on glass substrates. From reference 28, with the permission of AIP Publishing. (b) Stokes shift as a function of absorption edge and (c) FWHM of photoluminescence peak as a function of Cd concentration, from reference 27 copyright 2004 The Japan Society of Physics. (b) and (c) were measured on thin films grown by RPE-MOVPE on *a*-plane sapphire.

Concomitantly to this bandgap narrowing, the incorporation of Cd leads to a Stokes shift and a photoluminescence FWHM that increase with Cd content, as shown in Figures 4(b) and (c) respectively, and attain their maxima at a Cd content of about 30%. It is noteworthy that the maximum Stokes shift experimentally determined, 300meV-350meV, seems to be independent of the growth technique and substrate employed and might be, thus, intrinsic to ZnCdO:[18,26,35] for example, for ZnCdO thin films grown by MBE on ZnO substrates and emitting at about 2.55eV the Stokes shift is in the order of 300meV,[35] while it amounts to 313meV for PLD-grown ZnCdO thin films on *a*-sapphire and emitting in the same wavelength range.[18] In spite of the emission FWHM of ZnCdO alloys, numerous groups have fabricated single and multiple quantum wells based on ZnMgO or ZnO barriers, and with Cd contents in the ZnCdO wells ranging from some percents (4%-9%)[47,71,72,73] to more than 10%[20,44] and even more than 20%.[62,74] In general, the behavior of such heterostructures reproduces features already studied in other wurtzite systems: the presence of built-in internal electric fields in the order of some MV/cm due to the polarization discontinuity (spontaneous+piezoelectric) across the well/barriers interfaces,[75] which give rise to the quantum confined Stark effect;[76,77] an S-shaped[10,72,73] temperature dependence of the photoluminescence emission energy as observed in ZnCdO thin films,[39] with a relative energy minimum at low temperatures that becomes deeper the larger the Cd content is;[73] and a W-shaped temperature dependence of the emission FWHM.[71,72] While these last two observations are not specific to ZnCdO quantum wells and are also observed in ZnO/ZnMgO quantum wells and other materials combinations, the use of ZnCdO introduces larger potential fluctuations (and, thus, larger exciton localization) and increases the inhomogeneous broadening necessary to fit the experimental data.[71]

As will be discussed in the last section, for some time ZnO/ZnCdO multiple quantum wells were considered as possible active regions of vertical cavity surface emitting lasers working in the visible range. To design such complex heterostructures a good knowledge of the materials refractive index is necessary. For ZnCdO alloys the dispersion of the refractive index in the transparency region has been measured by ellipsometry[24,40] and by transmission[78] measurements. As shown in Figure 5, the refractive index grows as the energy approaches the bandgap edge and, most important in this context, for a given energy it increases with increasing Cd content[24,40,78], which is beneficial in terms of mode confinement and, thus, in terms of active region/cavity mode overlap.

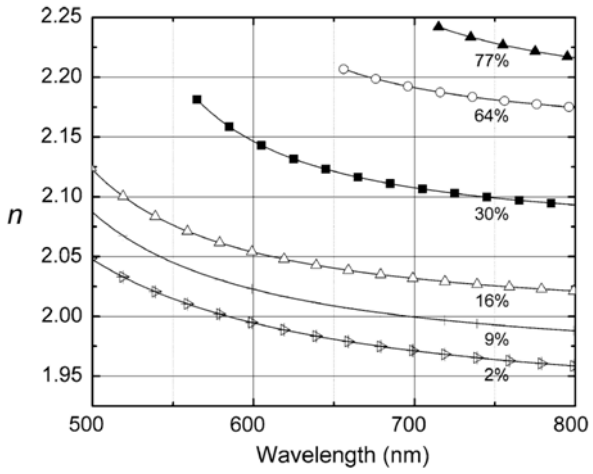

Figure 5: Real part of the refractive index as extracted from fitting experimental points (measured in transmission) to a Sellmeier dispersion model. ZnCdO thin films were grown by MBE on GaN-on-Sapphire templates. Note that the films corresponding to 64% and 77% Cd content might contain a mixture of crystalline phases.

Electronic properties of ZnCdO.

While the optical properties of ZnCdO alloys have been well established in the last years, only some studies have dealt with their electronic and electrical properties,[28,29,48,54,79] which results in still unsolved discrepancies.

This is particularly striking when considering the band alignment of ZnO/ZnCdO heterostructures and especially the corresponding bandoffsets.[29,48,54,79] In general, and even if some reports suggest a type-II band alignment,[79] a type-I band alignment ensuring carrier confinement of both electrons and holes is accepted,[29,54,79] consistent with quasiparticle electronic structure calculations (which make use of a cluster expansion to account for the wurtzite and rocksalt polymorphs, as discussed in the first section).[80] Differences appear when comparing the quantitative values of the conduction-band minimum offsets (ΔE_C) and valence-band maximum offsets (ΔE_V) as a function of Cd concentration as well as their ratio ($\Delta E_C/\Delta E_V$). The most complete study in terms of swept Cd composition has been carried out by Detert *et al*. [29] As shown in Figure 6, the conduction-band minimum displays a downward shift of about 600meV from pure ZnO to $Zn_{0.31}Cd_{0.69}O$, while the valence band maximum increases by about 1200meV, leading to total bandgap variation of about 1600meV in this composition range, consistent with optical measurements (see previous section). Furthermore, these measurements indicate that $\Delta E_C/\Delta E_V$ is Cd-dependent, eventually explaining why different authors report different values.[29,54,79] Figure 6 further suggests that the large bandgap tunability of ZnCdO stems from the sensitivity of the wurtzite valence band to Cd incorporation, an observation which is not reproduced yet by theoretical calculations[80] and for which a deeper knowledge of the exact valence band electronic structure is still necessary.[81] This is especially important for ZncdO alloys in the rocksalt phase, given their indirect character.[29,70,81]

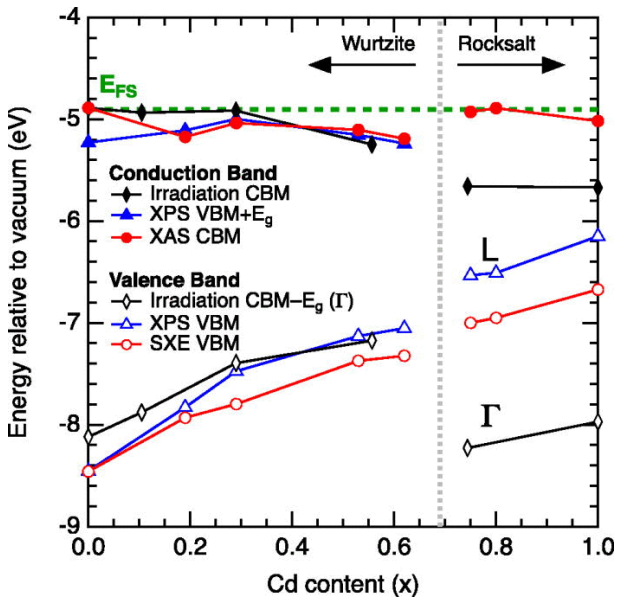

Figure 6: Band edge shifts as measured by irradiation-induced Fermi-level pinning, XPS and XAS/SXE, with band edge information inferred by incorporating the intrinsic bandgap for each Cd composition. Measurements were carried out on thin films deposited by pulsed filtered cathodic arc deposition on glass substrates. From reference 29, with the permission of AIP Publishing.

The authors in reference 29 point out that the slight dependence of the conduction-band minimum on Cd concentration (within the wurzite phase) is consistent with the weak composition

dependence of the electron mobility across the whole composition range (from 15cm^2/V·s for pure ZnO to 30 cm^2/V·s for $Zn_{0.31}Cd_{0.69}O$),[28] given that the strength of alloy disorder scattering is proportional to ΔE_C for a given Cd composition. Still, one should note that the polycrystalline nature of the ZnCdO thin films employed in this study might mask this dependence of the electron mobility on alloy composition. This point towards the need of accurate studies, similar to those in reference 29, but this time on single-crystalline ZnCdO thin films.

Towards ZnCdO-based devices

The wide wavelength range covered by ZnCdO alloys promised a number of applications, the most appealing ones being in the optoelectronic domain, including all-oxide multijunction solar cells, photodiodes, light-emitting devices and laser diodes.[82]

The first reports of lasing action in high-quality ZnCdO/ZnO quantum wells grown on *a*-plane sapphire and on O-polar ZnO substrates[36] were very promising, especially taking into account the simplicity of the structures in terms of mode confinement, as well as the large wavelength tunability (see Figure 7(a)). Furthermore, the relatively low lasing thresholds for first structures, in the order of some tens of kW/cm^2 (see inset in Figure 7b), suggested the possibility of easily reducing them by improving the photonic waveguides as well as the active regions, whose gain was shown to depend critically on the interplay between sheet carrier density and internal electrostatic fields.[83,84]

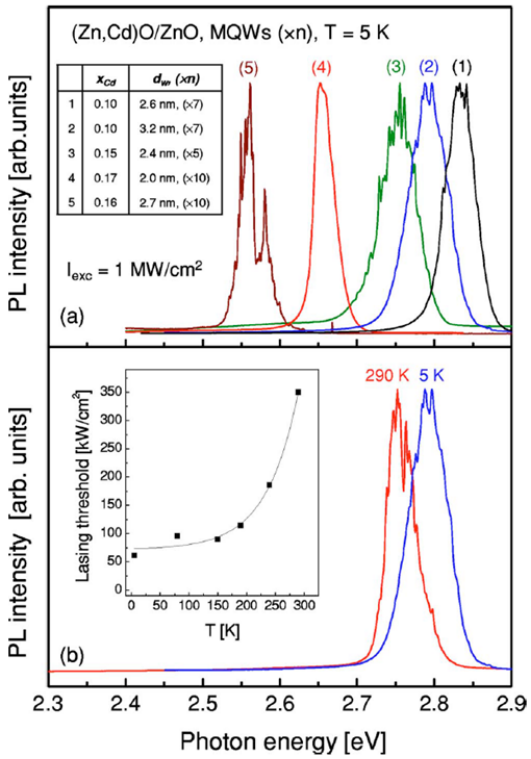

Figure 7: (a) Dependence of lasing wavelength on Cd concentration and on quantum well thickness. Structures 1-4 were grown on *a*-sapphire, while structure 5 was grown on O-polar ZnO substrate. (b) Lasing action from structure 2 in (a), for low and room-temperature. The inset shows the temperature dependence of the lasing threshold for this structure. From reference 36, with the permission of AIP Publishing.

The next step in the development of ZnCdO-based devices was to be the fabrication of electrically-injected devices, but this faced the extremely hard task of p-type doping ZnO,[85,86] which is

the simplest and probably best adapted electrical injector one can think of. Thus, even if there have been some reports in the use of Sb-doped ZnO as hole injector for ZnCdO,[87] alternative strategies employing other p-type materials have been tested. More precisely, Nakamura *et al*. employed a *p*-type 4H-SiC substrate, which exhibits the same wurtzite structure as ZnCdO and a relatively small lattice mismatch (0.5% with respect to pure ZnO), to inject holes into *n*-ZnMgO/nid n-ZnCdO/p-SiC heterostructures. The authors succeeded, by varying the Cd concentration, in fabricating electrically-injected LEDs emitting from blue to red passing through green.[88]

Still, the most tempting alternative to *p*-ZnO material would be the use of *p*-type nitrides, with a much more mature technology. In this context Mares and coworkers grew an n^+-ZnO/n-ZnMgO/nid-$Zn_{0.88}Cd_{0.12}O$ QW/p-GaN heterostructure.[89] However, their structure illustrates the problem encountered when combining these materials, as the heterojunction between the employed nitrides and oxides displays a type-II band alignment. Thus, spatially direct recombination of electrons and holes in the well coexists with spatially indirect recombination between electrons in the well and holes accumulated at the ZnCdO/p-GaN interface. And even if the optical direct transition is the most likely to occur, since the square overlap integral between the electron and hole wavefunctions within the quantum well amounts to 0.89, compared to about 0.15 for the other possible transitions, the large hole accumulation at the p-GaN/ZnCdO interface results in a significant contribution of the spatially indirect transitions. These two effects result in a current-dependent wavelength emission with spatially-indirect transitions being favored at larger current densities.

Unfortunately, none of the above-mentioned reports discusses efficiencies nor do they provide output powers, making difficult any fair comparison with their nitrides counterparts.

Conclusions

The promises predicted to ZnCdO required a precise control over the Cd concentration of ZnCdO as well as over its crystalline phase. After some years of research, the possibility of fabricating ZnCdO thin films spanning the whole composition range, and addressing individually each of its stable crystalline phases, enabled to study its intrinsic properties within the corresponding stability composition range. The wide bandgap tunability was rapidly demonstrated and numerous teams tried to exploit it in optoelectronic devices, namely light-emitting devices and laser diodes. However, similar to the situation encountered by ZnO, electrical injection has been shown to be extremely difficult, even when exploiting alternative materials as hole injectors.

Thus, the question about the future of ZnCdO needs to be posed. In the introduction we said that two applications were initially envisaged, either as active region in optoelectronic devices or as TCO. And while ZnCdO has already shown all its potentials in the first domain, whose future will be related to that of ZnO, it seems to the author that ZnCdO has still a word to say independently of ZnO in applications requiring TCOs. Indeed, its role as TCO might be played in pure from (i.e. as ZnCdO alone) or doped/alloyed with other elements. Whether these elements will be scandium, yttrium, magnesium, tin or indium only the future will tell us.

References

[1] C. Weisbuch, M. Piccardo, L. Martinelli, J. Iveland, J. Peretti, and J. S. Speck, Phys. Status Solidi A 212 (2015) 899.
[2] C. Klingshirn, R. Hauschild, H. Priller, M. Decker, J. Zeller, and H. Kalt, Superlattice Microst. 38 (2005) 209.
[3] T. Makino, Y. Segawa, M. Kawasaki, A. Ohtomo, R. Shiroki, K. Tamura, T. Yasuda, and H. Koinuma, Appl. Phys. Lett. 78 (2001) 1237.
[4] Y. S. Choi, C. G. Lee, and S. M. Cho, Thin Solid Films 289 (1996) 153.
[5] M. Kawasaki, A. Ohtomo, R. Shiroki, I. Ohkubo, H. Kimura, G. Isoya, T. Yasuda, Y. Segawa, and H. Koinuma, *Extended Abstracts of the 1998 International Conference on Solid State Devices and Materials* (Business Center, Academic Society of Japan, Hiroshima, Japan 1998), p. 356-357.
[6] T. Minami, Semicond. Sci. Technol. 20 (2005) S35.
[7] A. J. Freeman, K. R. Poeppelmeier, T. O. Mason, R. P. H. Chang, and T. J. Marks, MRS Bull. 25 (2000) 45.
[8] P. D. C. King, and T. D. Veal, J. Phys.: Condens. Matter 23 (2011) 334214.
[9] O. Madelung, U. Rössler, and M. Schulz, *Zinc oxide (ZnO) crystal structure, lattice parameters: Datasheet from Landolt-Börnstein - Group III Condensed Matter · Volume 41B: "II-VI and I-VII Compounds; Semimagnetic Compounds"* in SpringerMaterials and *Cadmium oxide (CdO) crystal structure, lattice parameters, thermal expansion: Datasheet from Landolt-Börnstein - Group III Condensed Matter · Volume 41B: "II-VI and I-VII Compounds; Semimagnetic Compounds"* in SpringerMaterials, Springer-Verlag (1999).
[10] T. Makino, C. H. Chia, N. T. Tuan, Y. Segawa, M. Kawasaki, A. Ohtomo, K. Tamura, and H. Koinuma, Appl. Phys. Lett. 77 (2000) 1632.
[11] K. Sakurai, T. Kubo, D. Kajita, T. Tanabe, H. Takasu, S. Fujita, and S. Fujita, Jpn. J. Appl. Phys. 39 (2000) L1146.
[12] K. Sakurai, T. Takagi, T. Kubo, D. Kajita, T. Tanabe, H. Takasu, S. Fujita, and S. Fujita, J. Cryst. Growth 237 (2002) 514.
[13] Th. Gruber, C. Kirchner, R. Kling, F. Reuss, A. Waag, F. Bertram, D. Forster, J. Christen, and M. Schreck, Appl. Phys. Lett. 83 (2003) 3290.
[14] F. Bertram, S. Giemsch, D. Forster, J. Christen, R. Kling, C. Kirchner, and A. Waag, Appl. Phys. Lett. 88 (2006) 061915.
[15] J. Zuniga-Perez, V. Munoz-Sanjosé, M. Lorenz, G. Benndorf, S. Heitsch, D. Spemann, and M. Grundmann, J. Appl. Phys. 99 (2006) 023514.
[16] X. J. Wang, I. A. Buyanova, W. M. Chen, M. Izadifard, S. Rawal, D. P. Norton, S. J. Pearton, A. Osinsky, J. W. Dong, and A. Dabiran, Appl. Phys. Lett. 89 (2006) 151909.
[17] I. A. Buyanova, J. P. Bergman, G. Pozina, W. M. Chen, S. Rawal, D. P. Norton, S. J. Pearton, A. Osinsky, and J. W. Dong, Appl. Phys. Lett. 90 (2007) 261907.
[18] M. Lange, C. P. Dietrich, K. Brachwitz, T. Böntgen, M. Lorenz, and M. Grundmann, J. Appl. Phys. 112 (2012) 103517
[19] A. Y. Azarov, T. C. Zhang, B. G. Svensson, and A. Y. Kutnetsov, Appl. Phys. Lett. 99 (2011) 111903
[20] S. Sadofev, S. Blumstengel, J. Cuiu, J. Puls, S. Rogaschewski, P. Schäfer, and F. Henneberge, Appl. Phys. Lett. 89 (2006) 201907
[21] J. Zuniga-Perez, C. Munuera, C. Ocal, and V. Munoz-Sanjose, J. Cryst. Growth 271 (2004) 223.
[22] J. Zuniga-Perez, C. Martinez-Tomas, and V. Munoz-Sanjose, phys. stat. sol. c 2 (2005) 1233.
[23] J. Ishihara, A. Nakamura, S. Shigemori, T. Aoki, and J. Temmyo, Appl. Phys. Lett. 89 (2006) 091914
[24] T. Ohashi, K. Yamamoto, A. Nakamura, T. Aoki, and J. Temmyo, Jpn. J. Appl. Phys. 46 (2007) 2516
[25] A. Nakamura, S. Shigemori, Y. Shimizu, T. Aoki, A. Tanaka, and J. Temmyo, Jpn. J. Appl. Phys. 42 (2003) L775
[26] S. Shigemori, A. Nakamura, J. Ishihara, T. Aoki, and J. Temmyo, Jpn. J. Appl. Phys. 43 (2004) L1088.
[27] A. Nakamura, J. Ishihara, S. Shigemori, K. Yamamoto, T. Aoki, H. Gotoh, and J. Temmyo, Jpn. J. Appl. Phys. 43 (2004) L1452
[28] D. M. Detert, S. H. M. Lim, K. Tom, A. V. Luce, A. Anders, O. D. Dubon, K. M. Yu, and W. Walukiewicz, Appl. Phys. Lett. 102 (2013) 232103.
[29] D. M. Detert, K. B. Tom, C. Battaglia, J. D. Denlinger, S. H. M. Lim, A. Javey, A. Anders, O. D. Dubon, K. M. Yu, and W. Walukiewicz, J. Appl. Phys. 115 (2014) 233708.
[30] Y. Chen, S. Zhang, W. Gao, F. Ke, J. Yan, B. Saha, C. Ko, J. Suh, B. Chen, J. W. Ager III, W. Walukiewicz, R. Jeanloz, and J. Wu, Appl. Phys. Lett. 108 (2016) 152105
[31] M. Sanati, G. L. W. Hart, and A. Zunger, Phys. Rev. B 68 (2003) 155210
[32] X. F. Fan, H. D. Sun, Z. X. Shen, J. L. Kuo, and Y. M. Lu, J. Phys.: Condens. Matter 20 (2008) 235221.

[33] Y. Z. Zhu, G. D. Chen, H. Ye, A. Walsh, C. Y. Moon, and S. H. Wei, Phys. Rev. B 77 (2008) 245209.
[34] A. Schleife, M. Eisenacher, C. Rödl, F. Fuchs, J. Furthmüller, and F. Bechstedt, Phys. Rev. B 81 (2010) 245210.
[35] S. Sadofev, P. Schäfer, Y. H. Fan, S. Blumstengel, F. Henneberger, D. Schulz, and D. Klimm, Appl. Phys. Lett. 91 (2007) 201923
[36] S. Sadofev, S. Kalusniak, J. Puls, P. Schäfer, S. Blumstengel, and F. Henneberger, Appl. Phys. Lett. 91 (2007) 231103.
[37] L. Li, Z. Yang, Z. Zuo, J. H. Lim, and J. L. Liu, Appl. Surf. Sci. 256 (2010) 4734.
[38] K. F. Chien, W. L. Shu, A. J. Tzou, Y. C. Lin, W. C. Chou, L. Lee, C. H. CHia, and C. S. Yang, J. Cryst. Growth 378 (2013) 208
[39] T. Y. Wu, Y. S. Huang, S. Y. Hu, Y. C. Lee, K. K. Tiong, C. C. Chang, J. L. Shen, and W. C. Chou, Solid State Commun. 237 (2016) 1
[40] C. Sartel, N. Haneche, C. Vilar, G. Amiri, J. M. Laroche, F. Jomard, A. Lusson, P. Galtier, V. Sallet, C. Couteau, J. Lin, R. Aad, and G. Lérondel, J. Vac. Sci. Technol. A 29 (2011) 03A114
[41] V. Venkatachalapathy, A. Galeckas, M. Trunk, T. Zhang, A. Azarov, and A. Y. Kuznetsov, Phys. Rev. B 83 (2011) 125315.
[42] M. A. Boukadhaba, A. Fouzri, C. Saidi, N. Sakly, A. Souissi, A. Bchetnia, C. Sartel, V. Sallet, and M. Oumezzine, J. Cryst. Growth 395 (2014) 14
[43] A. Nakamura, J. Ishihara, S. Shigemori, K. Yamamoto, T. Aoki, H. Gotoh, and J. Temmyo, Jpn. J. Appl. Phys. 44 (2005) L4
[44] K. Yamamoto, M. Adachi, T. Tawara, H. Gotoh, A. Nakamura, and J. Temmyo, J. Cryst. Growth 312 (2010) 1496
[45] K. Yamamoto, T. Tsuboi, T. Ohashi, T. Tawara, H. Gotoh, A. Nakamura, and J. Temmyo, J. Cryst. Growth 312 (2010) 1703
[46] M. Lange, C. P. Dietrich, G. Benndorf, M. Lorenz, J. Zuniga-Perez, and M. Grundmann, J. Cryst. Growth 328 (2011) 13.
[47] W. F. Yang, B. Liu, R. Chen, L. M. Wong, S. J. Wang, and H. D. Sun, Appl. Phys. Lett. 97 (2010) 061911.
[48] V. Devi, M. Kumar, R. J. Choudhary, D. M. Phase, R. Kumar, and B. C. Joshi, J. Appl. Phys. 117 (2015) 225305.
[49] J. Jiang, L. P. Zhu, H. P. He, Y. Li, Y. M. Guo, L. Cao, Y. G. Li, K. W. Wu, L. Q. Zhang, and Z. Z. Ye, J. Appl. Phys. 112 (2012) 083513.
[50] T. Liu, D. Wang, F. Guo, S. Jiao, J. Wang, Y. Liu, C. Luan, W. Cao, and L. Zhao, Superlattice Microst. 97 (2016) 569
[51] R. Zhang, P. Chen, Y. Zhang, X. Ma, and D. Yang, J. Cryst. Growth 312 (2010) 1908.
[52] X. Ma, P. Chen, R. Zhang, and D. Yang, J. Alloys and Compounds 509 (2011) 6599.
[53] O. Vigil, L. Vaillant, F. Cruz, G. Santana, A. morales-Acevedo, and G. Contreras-Puente, Thin Solid Films 361 (2000) 53.
[54] H. H. C. Lai, V. L. Kuznetsov, R. G. Egdell, and P. P. Edwards, Appl. Phys. Lett. 100 (2012) 072106.
[55] Z.L. Wang, J. Phys-Condens. Mat. **16**, R829-R858 (2004).
[56] G.C. Yi, C. Wang, and W.I Park, Semicond. Sci. Technol. **20**, S22-S34 (2005).
[57] M. Lorenz, A. Rahm, B. Cao, J. Zuniga-Perez, E. M. Kaidashev, N. Zhakarov, G. Wagner, T. Nobis, C. Czekalla, G. Zimmermann, and M. Grundmann, phys. stat. sol. b 247 (2010) 1265
[58] Q. Wan, Q. H. Li, Y. J. Chen, T. H. Wang, X. L. He, X. G. Gao, and J. P. Li, Appl. Phys. Lett. 84 (2004) 3085.
[59] F. Z. Wang, Z. Z. Ye, D. W. Ma, L. P. Zhu, F. Zhuge, and H. P. He, Appl. Phys. Lett. 87 (2005) 143101.
[60] F. Z. Wang, H. P. He, Z. Z. ye, and L. P. Zhu, J. Appl. Phys. 98 (2005) 084301.
[61] F. Z. Wang, Z. Z. Ye, D. Ma, L. Zhu, and L. P. Zhu, J. Cryst. Growth 283 (2005) 373.
[62] C. P. Dietrich, M. Lange, M. Stölzel, and M. Grundmann, Appl. Phys. Lett. 100 (2012) 031110.
[63] S. Chu, and G. Wang, Mat. Lett. 85 (2012) 149.
[64] M. Lopez-Ponce, A. Hierro, J. M. Ulloa, P. Lefbvre, E. Munoz, S. Agouram, V. Munoz-Sanjosé, K. Yamamoto, A. Nakamura, and J. Temmyo, Appl. Phys. Lett. 102 (2013) 143103.
[65] M. Lopez-Ponce, A. Nakamura, M. Suzuki, J. Temmyo, S. Agouram, M. C. Martinez-Tomas, V. Munoz-Sanjosé, P. Lefebvre, J. M. Ulloa, E. Munoz, and A. Hierro, Nanotech. 25 (2014) 255202
[66] S. M. Zhou, X. H. Zhang, X. M. Meng, S. K. Wu, and S. T. Lee, Mater. Res. Bull. 41 (2006) 340
[67] O. Lupan, T. Pauporté, T. Le Bahers, I. Ciofini, and B. Viana, J. Phys. Chem. C 115 (2011) 14548.
[68] J. A. Van Vechten, and T. K. Bergstresser, Phys. Rev. B 1 (1970) 3351.
[69] R. J. Guerrero-Moreno, and N. Takeuchi, Phys. Rev. B 66 (2002) 205205.
[70] P. H. Jefferson, S. A. Hatfield, T. D. Veal, P. D. C. king, C. F. McConville, J. Zuniga-Perez, and V. Munoz-Sanjosé, Appl. Phys. Lett. 92 (2006) 022101

[71] T. Makino, K. Saito, A. Ohtomo, M. Kawsaki, R. T. Senger, and K. K. Bajaj, J. Appl. Phys. 99 (2006) 066108
[72] W. F. Yang, L. M. Wong, S. J. Wang, H. D. Sun, C. H. Ge, A. Y. S. Lee, and H. Gong, Appl. Phys. Lett. 98 (2011) 121903
[73] W. F. Yang, R. Chen, B. Liu, L. M. Wong, S. J. Wang, H. D. Sun, Gong, J. Appl. Phys. 109 (2011) 113521
[74] S. Kalusniak, S. Sodfev, J. Puls, H. J. Wunsche, and F. Henneberger, Phys. Rev. B 77 (2008) 113312
[75] M. Grundmann, and J. Zuniga-Perez, Phys. Stat. Sol. b 253 (2016) 351
[76] M. Leroux, N. Grandjean, J. Massies, B. Gil, P. Lefebvre, and P. Bigenwald, Phys. Rev. B 60 (1999) 1496
[77] C. Morhain, T. Bretagnon, P. Lefebvre, X. Tang, P. Valvin, T. Guillet, B. Gil, T. Taliercio, M. Teisseire-Doninelli, B. Vinter, and C. Deparis, Phys. Rev. B 72 (2005) 241305
[78] J. W. Mares, M. Falanga, W. R. Folks, G. Boreman, A. Osinsky, B. Hertog, J. Q. Xie, and W. V. Schoenfeld, J. Electron. Mater. 37 (2008) 1665
[79] J. J. Chen, F. Ren, Y. Li, D. P. Norton, S. J. Pearton, A. Osinsky, J. W. Dong, P; P. Chow, and J. F. Weaver, Appl. Phys. Lett. 87 (2005) 192106
[80] A. Schleife, C. Rödl, J. Furthmüller, and F. Bechstedt, New J. of Phys. 13 (2011) 085012
[81] P. D. C. King, T. D. Veal, A. Schleife, J. Zuniga-Perez, B. Martel, P. H. Jefferson, F. Fuchs, V. Munoz-Sanjose, F. Bechstedt, and C. F. McConville, Phys. rev. B 79 (2009) 205205
[82] US Patent, US20100032008 A1, « Zinc oxide multi-junction photovoltaic cells and optoelectronic devices".
[83] S. H. Park, and D. Ahn, Appl. Phys. Lett. 94 (2009) 083507
[84] H. C. Jeon, S. H. Park, S. J. Lee, T. W. Kang, and T. F. George, Appl. Phys. Lett. 96 (2010) 101113
[85] A. Tsukazaki, A. Ohtomo, T. Onuma, M. Ohtani, T. Makino, M. Sumiya, K. Ohtani, S. F. Chichibu, S. Fuke, Y. Segawa, H. Ohno, H. Koinuma, and M. Kawasaki, Nature Mater. 4 (2005) 42
[86] K. Nakahara, S. Akasaka, H. Yuji, K. Tamura, T. Fujii, Y. Nishimoto, D. Takamizu, A. Sasaki, T. Tanabe, H. Takasu, H. Amaike, T. Onuma, S. F. Chichibu, A. Tsukazaki, A. Ohtomo, and M. Kawasaki, Appl. Phys. Lett. 97 (2010) 013501
[87] L. Li, Z. Yang, J. Y. Kong, and J. L. Liu, Appl. Phys. Lett. 95 (2009) 232117
[88] A. Nakamura, T. Ohashi, K. Yamamoto, J. Ishihara, T. Aoki, J. Temyo, and H. Gotoh, Appl. Phys. Lett. 90 (2007) 093512
[89] J. W. Mares, M. Falanga, A. V. Thompson, A. Osinsky, J. Q. Xie, B. Hertog, A. Dabiran, P. P. Chow, S. Karpov, and W. V. Schoenfeld, J. Appl. Phys. 104 (2008) 093107